

Analysis of Degree of Polarization as a Control Signal in PMD Compensation Systems Aided by Polarization Scrambling

Majid Safari, *Student Member, IEEE*, and Amir Ahmad Shishegar, *Member, IEEE*

Abstract—The performance of degree of polarization (DOP) is investigated as a control signal in polarization-mode dispersion (PMD) compensation systems aided by polarization scrambling. The relation between the input and output polarization states of a signal propagating through a polarization scrambler and a PMD-induced optical fiber is described by a 3×3 Stokes transfer matrix. The average DOP of the output signal over a period of polarization scrambling is derived as an alternative to the conventional DOP-based control signal, i.e., minimum DOP. In the presence of first- and all-order PMDs, the performance of the average and minimum DOPs in monitoring of differential group delay (DGD) for different data formats (i.e., RZ and NRZ) is evaluated. The performance of the two control signals are further investigated by calculating the outage probability of a feedforward first-order PMD compensation system. The results show that the average DOP outperforms the minimum DOP and also gives a wider DGD monitoring range.

Index Terms—Degree of polarization (DOP), optical communication systems, polarization-mode dispersion (PMD), polarization scrambling.

I. INTRODUCTION

POLARIZATION-MODE dispersion (PMD) is one of the most important degradation factors of fiber-optic transmission systems. Pulse broadening due to PMD limits the length and the bit rate of optical communication links. PMD is introduced by differential group delay (DGD), which is a frequency-dependent delay between two orthogonal principal states of polarization (PSPs). Time-varying and stochastic effects of PMD lead to system outages frequently, thus it should be adaptively compensated by monitoring of the instantaneous DGD.

PMD compensators commonly use feedback or feedforward schemes to provide control signals for adaptive and automatic compensation. Feedback compensation schemes can be used to mitigate high-order PMD effects, but they are complex and may be trapped in sub-optimum conditions [1]–[5]. On the other

hand, the feedforward schemes are simple and fast, but require polarization scrambling at the transmitter [6]–[8]. Polarization scrambling is a valuable technique which improves the reliability of DGD estimation in both feedforward and feedback PMD compensators [3]–[8]. PMD monitoring signals commonly obtained from the RF spectrum of the received signal [2], [3] or using the signal's degree of polarization (DOP) [4]–[8]. DOP-based control signals are bit-rate independent and can be easily utilized in PMD compensation systems, but polarization scrambling is required for a reliable PMD monitoring due to the dependence of DOP on input state of polarization (SOP).

When an optical signal is affected by PMD, the output SOP changes over the frequency spectrum and DOP decreases. The relationship between DOP, all-order PMD and the optical power spectrum in the Jones space has been previously obtained in [9] but only for a certain input SOP. This relationship has been also described with a different formulation in [10] using second-order PMD approximation. However, the role of polarization scrambling in DOP evaluation is neglected in both papers.

In this paper, we investigate the performance of DOP as a control signal in PMD compensation systems using polarization scrambling at the transmitter. First, the relationship between DOP, all-order PMD, and optical power spectrum is demonstrated in the Jones space for any arbitrary input SOP. The relation between the input and output SOP of a scrambled signal launched into a PMD-induced fiber is described as a Stokes transfer matrix. The average DOP is introduced as an alternative control signal for DGD monitoring to the minimum DOP. Analytical expressions are given for the average DOP in the presence of first- and all-order PMDs. The DGD monitoring performance of the two control signals are characterized in the presence of first and all-order PMDs. Finally, the outage probability of a first-order PMD compensator for the two different DOP-based control signals is calculated to compare their PMD monitoring performances in a feedforward configuration.

II. DOP FOR A SCRAMBLED SIGNAL

We first modify the analytical expression presented in [9] for calculating the DOP of a signal with a certain input SOP ($\hat{e}_{in} = [0 \ 1]^T$), to the case that the input signal is scrambled and could have any arbitrary instantaneous SOP ($\hat{e}_{in} = [\cos(\theta) \exp(j\varphi) \ \sin(\theta)]^T$). Fig. 1 shows the block diagram of a DOP-based PMD monitoring system for the feedforward PMD compensation. In Fig. 1, PC (polarization controller) realizes the effects of polarization scrambling. The Jones transfer

Manuscript received March 09, 2006; revised October 05, 2007. Current version published October 24, 2008. This work was supported in part by the Iran Telecommunication Research Center (ITRC).

M. Safari was with the Advanced Communication Research Institute (ACRI), Department of Electrical Engineering, Sharif University of Technology, Tehran, Iran. He is currently with the Department of Electrical and Computer Engineering, University of Waterloo, Waterloo, ON N2L 3G1, Canada (e-mail: m3safari@uwaterloo.ca).

A. A. Shishegar is with the Advanced Communication Research Institute (ACRI), Department of Electrical Engineering, Sharif University of Technology, Tehran, Iran (e-mail: shishegar@sharif.ir).

Digital Object Identifier 10.1109/JLT.2007.914516

matrices of PC and the optical fiber affected by PMD can be expressed as [1], [9]

$$P = \begin{bmatrix} \cos(\theta)e^{j\varphi} & -\sin(\theta) \\ \sin(\theta) & \cos(\theta)e^{-j\varphi} \end{bmatrix} \quad (1)$$

and

$$T(\omega) = e^{(-\alpha(\omega)L - j\beta(\omega)L)}U(\omega) \quad (2)$$

where θ and φ are the time-varying angles which describe the instantaneous SOP of the scrambled signal. $\alpha(\omega)$, $\beta(\omega)$, and L are the attenuation, the mean propagation constant, and the length of the fiber, respectively. In (2), $U(\omega)$ is the unitary matrix which can be written as

$$U(\omega) = \begin{bmatrix} u_1 & u_2 \\ -u_2^* & u_1^* \end{bmatrix}. \quad (3)$$

As it is illustrated in Fig. 1, The PC block has been inserted to scramble the polarization of the signal launched into the fiber by changing the input SOP of the signal over the Poincaré sphere. Therefore, the total unitary matrix of the link including the inserted polarization controller can be expressed in the form of $U(\omega)$ as

$$U_{\text{tot}}(\omega) = U(\omega)P = \begin{bmatrix} \bar{u}_1 & \bar{u}_2 \\ -\bar{u}_2^* & \bar{u}_1^* \end{bmatrix} \quad (4)$$

where \bar{u}_1 and \bar{u}_2 are

$$\begin{aligned} \bar{u}_1 &= u_1 \cos(\theta) \exp(j\varphi) + u_2 \sin(\theta) \\ \bar{u}_2 &= u_2 \cos(\theta) \exp(-j\varphi) - u_1 \sin(\theta). \end{aligned} \quad (5)$$

At the output of polarimeter, the instantaneous DOP of the scrambled signal can be expressed in terms of the output Stokes parameters of the signal as [9]

$$\text{DOP}(\theta, \varphi) = \frac{\sqrt{S_{1\text{out}}^2 + S_{2\text{out}}^2 + S_{3\text{out}}^2}}{S_{0\text{out}}} \quad (6)$$

where $S_{0\text{out}} = \int_{-\infty}^{+\infty} S_{\text{out}}(\omega) d\omega$ is the output signal's power and $S_{\text{out}}(\omega)$ is the output signal's power spectrum. In (6), $S_{1\text{out}}(\omega)$, $S_{2\text{out}}(\omega)$, and $S_{3\text{out}}(\omega)$ are the output Stokes parameters measured by polarimeter which were previously derived in [9] for the certain input SOP of $[1 \ 0]^T$ in the Jones space or equivalently $[1 \ 0 \ 0]^T$ in the Stokes space. Substituting the coefficients of the unitary matrix (3) with the coefficients of the total unitary matrix (4) in the Stokes parameter expressions derived in [9] and modifying the sign of the second and third Stokes parameters (i.e., $S_{2\text{out}}(\omega)$, and $S_{3\text{out}}(\omega)$) as discussed in the Appendix, the instantaneous output Stokes parameters of the scrambled signal can be obtained as

$$S_{1\text{out}} = \left\langle |u_1 \cos(\theta) e^{j\varphi} + u_2 \sin(\theta)|^2 - |u_2 \cos(\theta) e^{-j\varphi} - u_1 \sin(\theta)|^2 \right\rangle \quad (7)$$

$$S_{2\text{out}} = -1 \times \left\langle \text{Re}(2u_1 u_2 \cos(2\theta) + u_2^2 \sin(2\theta) e^{-j\varphi} - u_1^2 \sin(2\theta) e^{j\varphi}) \right\rangle \quad (8)$$

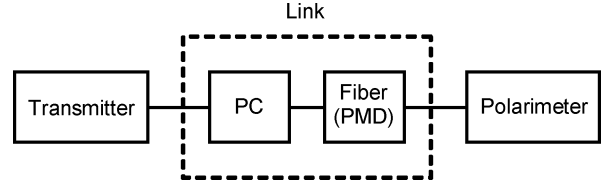


Fig. 1. Block diagram of a DOP-based PMD monitoring system for the feed-forward PMD compensation.

$$S_{3\text{out}} = -1 \times \left\langle \text{Im}(2u_1 u_2 \cos(2\theta) + u_2^2 \sin(2\theta) e^{-j\varphi} - u_1^2 \sin(2\theta) e^{j\varphi}) \right\rangle \quad (9)$$

where the bracket notation indicates the integration over the output signal's power spectrum so that $\langle \cdot \rangle = \int_{-\infty}^{+\infty} (\cdot) S_{\text{out}}(\omega) d\omega$.

By the left-circular definition of the Stokes space [11], the instantaneous input Stokes parameters of the scrambled signal before launching into the fiber are also given by

$$\begin{aligned} S_{1\text{in}} &= S_{0\text{in}} \cos(2\theta) \\ S_{2\text{in}} &= S_{0\text{in}} \sin(2\theta) \cos(\varphi) \\ S_{3\text{in}} &= S_{0\text{in}} \sin(2\theta) \sin(\varphi) \end{aligned} \quad (10)$$

where $S_{0\text{in}}$ is the input signal's power. Using (7)–(10), we can relate the input and output Stokes vectors of a scrambled signal using a 3×3 transfer matrix \mathbf{M} as

$$\mathbf{S}_{\text{out}} = \frac{1}{S_{0\text{in}}} \mathbf{M} \mathbf{S}_{\text{in}} \quad (11)$$

where \mathbf{S}_{in} and \mathbf{S}_{out} are the input and output Stokes vectors representing the SOP of the signal at the input and output of the fiber. In (11), \mathbf{M} can be expressed as

$$\mathbf{M} = \text{Re} \begin{bmatrix} \langle |u_1^2| - |u_2^2| \rangle & \langle 2u_1^* u_2 \rangle & \langle 2ju_2^* u_1 \rangle \\ -\langle 2u_1 u_2 \rangle & \langle u_1^2 - u_2^2 \rangle & \langle ju_1^2 + ju_2^2 \rangle \\ \langle 2ju_1 u_2 \rangle & \langle ju_2^2 - ju_1^2 \rangle & \langle u_1^2 + u_2^2 \rangle \end{bmatrix}. \quad (12)$$

In the case of first-order PMD, we assume that the fast PSP of the fiber is aligned with the polarization state corresponds to $[1 \ 0]^T$ in the Jones space. Thus, the unitary transform matrix of the fiber reduces to

$$U(\omega) = \begin{bmatrix} e^{j\omega \text{DGD}/2} & 0 \\ 0 & e^{-j\omega \text{DGD}/2} \end{bmatrix}. \quad (13)$$

Using (6) and (11)–(13), the instantaneous DOP (θ, φ) for the case of first-order PMD is readily expressed as

$$\text{DOP} = \sqrt{\cos^2(2\theta) + \sin^2(2\theta) \frac{\langle \cos(\omega \text{DGD}) \rangle^2}{S_{0\text{out}}^2}}. \quad (14)$$

A. Minimum DOP as a Control Signal

In DOP-based PMD compensation systems aided by polarization scrambling, the signal is scrambled by a scrambler at the transmitter and the DOP is measured by a polarimeter at the receiver. Then the control signal is obtained from the DOP

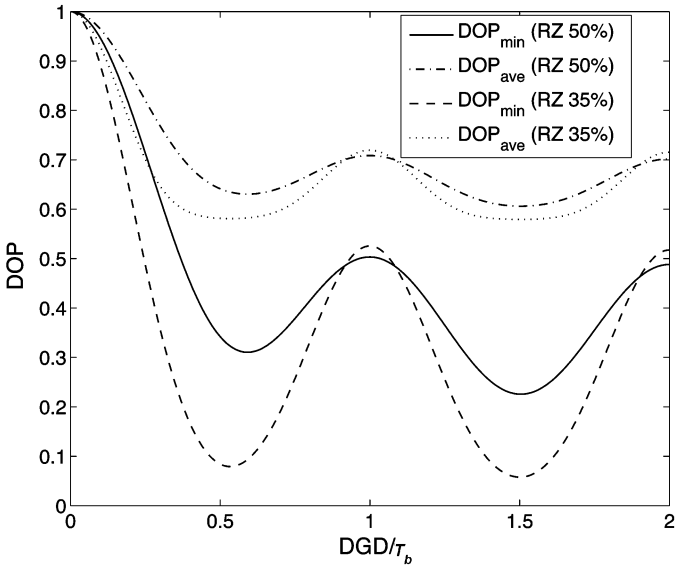


Fig. 2. The minimum and average DOPs versus DGD to the bit time in the presence of first-order PMD for RZ input signals.

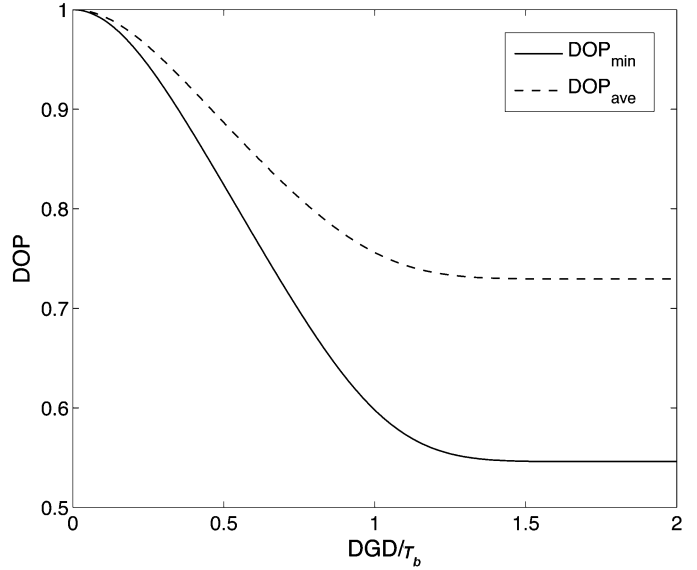


Fig. 3. The minimum and average DOPs versus DGD to the bit time in the presence of first-order PMD for NRZ input signals.

samples taken during a complete scrambling period over the Poincaré sphere [4]–[8]. Applying the minimum DOP sample as a control signal for the DGD monitoring, maximizes the sensitivity of DOP to DGD; however, since only a single sample is used, the control signal is strongly affected by the polarimeter noise [5]. This noise can be reduced by two methods. Using a more accurate polarimeter can reduce the measurement noise of each sample and increasing the number of measurement samples can reduce the noise of the discrete search. But these two methods make compensator more expensive and slow.

The minimum DOP (DOP_{\min}) can be obtained by minimizing $DOP(\theta, \varphi)$ with respect to the instantaneous input polarization angles (i.e., θ and φ). The analytical solution for DOP_{\min} in the presence of all-order PMD is too complicated, but it can be obtained numerically by calculating (6) in several polarization states which cover the entire Poincaré sphere uniformly and then finding the minimum sample. However, for the case of first-order PMD, there is a simple analytical solution for DOP_{\min} obtained by minimizing (14) with respect to θ which was previously reported in [9] as

$$DOP_{\min} = \frac{\langle \cos(\omega DGD) \rangle}{S_{0\text{out}}}. \quad (15)$$

B. Average DOP as a Control Signal

Recently, an average value of DOP measurement samples during one period of polarization scrambling has been pro-

posed to be used as a control signal in PMD compensation systems. This method reduces the fluctuation of data caused by polarimeter noise at the cost of reducing the DOP sensitivity to DGD [5]. Thus, there is an advantage (reducing polarimeter noise effects) and a disadvantage (reducing the DOP sensitivity) in using average DOP as a control signal compared with the minimum DOP. The average DOP can be defined as

$$DOP_{\text{ave}} = \sqrt{E\{DOP^2(\theta_i, \varphi_i)\}} \quad (16)$$

where θ_i and φ_i are defined as random variables with uniform distribution in the intervals $[0, \pi/2]$ and $[0, 2\pi]$, respectively, to ensure that the Poincaré sphere is entirely covered by polarization scrambling. The notation $E\{\cdot\}$ which indicates statistical averaging, can be expressed as

$$E\{\cdot\} = \frac{1}{2\pi} \int_0^{2\pi} \int_0^{\pi/2} (\cdot) \sin(2\theta) d\theta d\varphi. \quad (17)$$

Using (6), (16), and (17), DOP_{ave} in the presence of all-order PMD can be obtained as shown in (18) at the bottom of the page. Inserting (13) into (18) the DOP_{ave} in the presence of first-order PMD is also obtained as

$$DOP_{\text{ave}} = \sqrt{\frac{1}{3} + \frac{2\langle \cos(\omega DGD) \rangle^2}{3S_{0\text{out}}^2}}. \quad (19)$$

$$DOP_{\text{ave}} = \sqrt{\frac{\langle |u_1|^2 - |u_2|^2 \rangle^2 + 2(\langle \text{Re}(u_1^2) \rangle^2 + \langle \text{Im}(u_1^2) \rangle^2 + \langle \text{Im}(u_2^2) \rangle^2 + \langle \text{Re}(u_2^2) \rangle^2) + 4(\langle \text{Im}(u_1 u_2) \rangle^2 + \langle \text{Re}(u_1 u_2) \rangle^2 + \langle \text{Re}(u_1^* u_2) \rangle^2 + \langle \text{Im}(u_1^* u_2) \rangle^2)}{3S_{0\text{out}}^2}}. \quad (18)$$

III. DOP-BASED DGD MONITORING IN THE PRESENCE OF FIRST-ORDER PMD

Figs. 2 and 3 show the comparison between the numerical results of the minimum and average DOPs versus DGD/T_b (DGD relative to the bit time) in the presence of first-order PMD using RZ and NRZ input signals, respectively. 40 Gb/s input signals are generated using the pseudorandom bit sequences (PRBS) of Gaussian RZ pulses and super-Gaussian ($m = 2$) NRZ pulses with word length of $2^5 - 1$. The RZ pulses are considered with different duty-factors (i.e., full width at half maximum duration to the bit time ratio).

Fig. 2 shows that for RZ signals, there is a defined limit to DGD monitoring range for both DOP_{\min} and DOP_{ave} at the point that the measured DOP reaches its first minimum value. The existence of this first-order limit was previously reported for DOP_{\min} in [9]. For NRZ signals, the DGD monitoring range is also limited due to the lack of the DOP sensitivity to DGD, as DGD exceeds the pulse width (Fig. 3). As aforementioned, the sensitivity of DOP_{\min} to DGD is greater than the sensitivity of DOP_{ave} . Moreover, the DOP sensitivity to DGD decreases when the duty factor of the input pulses increases for RZ signals.

IV. DOP-BASED DGD MONITORING IN THE PRESENCE OF ALL-ORDER PMD

We use Orlandini's analytical model [12] for PMD simulation to investigate the DOP degradation of a scrambled signal induced by all-order PMD. Discrete random wave-plate (DRW) model is a more common numerical model for PMD simulation [13]. However, for a fiber with a certain mean DGD, a complete statistical realization of the high DGD states can not be generated using DRW model [10]. On the other hand, Orlandini's model provides complete statistical realizations of the fiber for any DGD values. This model needs only two parameters with known statistics, the fiber DGD and the PSP depolarization rate. It is the most precise analytical model of representing the unitary matrix coefficients as reported in [12] and [13]. The analytical expressions for calculating the unitary matrix coefficients, in this model, were obtained by solving the differential equation that relates the unitary matrix and PMD vector. This solution was determined by assuming that the PMD vector has a constant magnitude and rotates with an angular velocity on a circumference in the Stokes space [12].

To study the performance of the DOP-based DGD monitoring scheme, for each DGD state, the DOP_{\min} and DOP_{ave} are calculated for 10 000 independent realizations of a fiber. These independent realizations are generated by a random PSP depolarization rate with mean square value of $\pi DGD^2/6$ and using probability distribution function reported in [14]. Then the mean (Figs. 4 and 5) and the standard deviation (Figs. 6 and 7) of DOP_{\min} and DOP_{ave} over different realizations of the fiber are obtained.

Figs. 4 and 5 show the comparison between the minimum and average DOPs versus DGD to the bit time in the presence of all-order PMD using RZ and NRZ input signals, respectively. The results show that the range of DOP variation is increased due to the higher order PMD effects. The first-order limit to the DGD monitoring range (i.e., first minimum point for RZ pulses

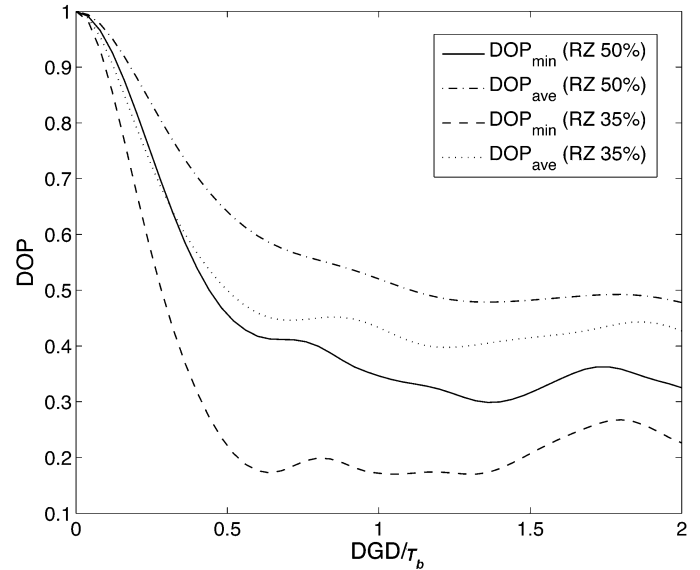


Fig. 4. The minimum and average DOPs versus DGD to the bit time in the presence of all-order PMD for RZ input signals.

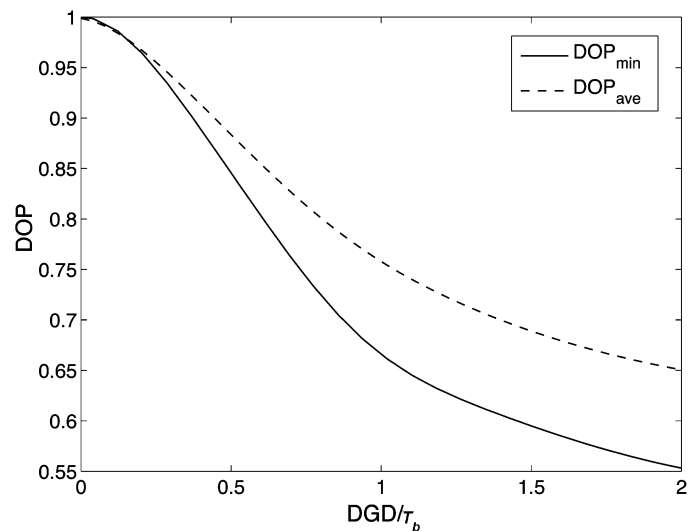


Fig. 5. The minimum and average DOPs versus DGD to the bit time in the presence of all-order PMD for NRZ input signals.

and lack of DOP sensitivity for NRZ pulses) is shifted to the larger DGD values. Figs. 6 and 7 show the comparison between the standard deviation of the minimum and average DOPs versus DGD to the bit time in the presence of all-order PMD using RZ and NRZ input signals, respectively. The standard deviation of DOP, for each DGD value, reflects the amount of ambiguity in DGD monitoring. A higher-order limit to DGD monitoring range can be defined at the DGD point that this ambiguity (i.e., standard deviation of DOP) exceeds a threshold given for the PMD compensation system. We can use this high-order limit as a criterion to compare the DGD monitoring range of the two control signals. The comparison shows less ambiguous DGD monitoring for the DOP_{ave} considering different input signals. Therefore, the wider DGD monitoring range is another advantage of using DOP_{ave} as an alternative to DOP_{\min} in addition to its low-sensitivity to the polarimeter noise.

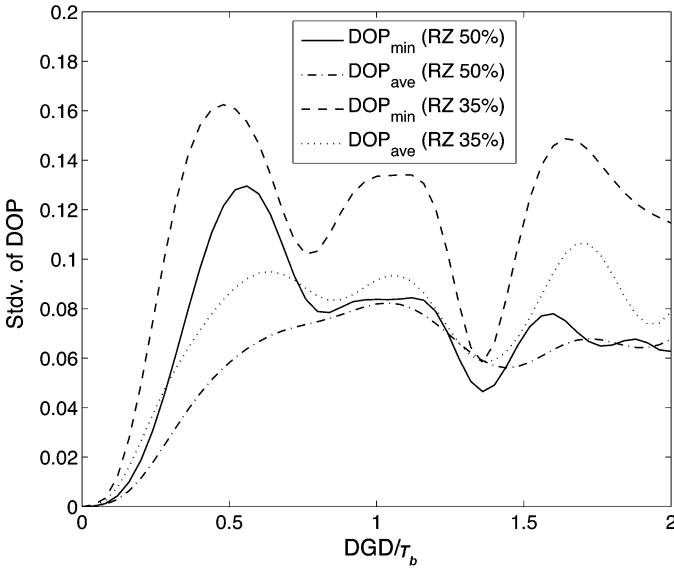


Fig. 6. Comparison of the standard deviation of the minimum and average DOPs versus DGD to the bit time in the presence of all-order PMD using RZ input signals with different duty factors.

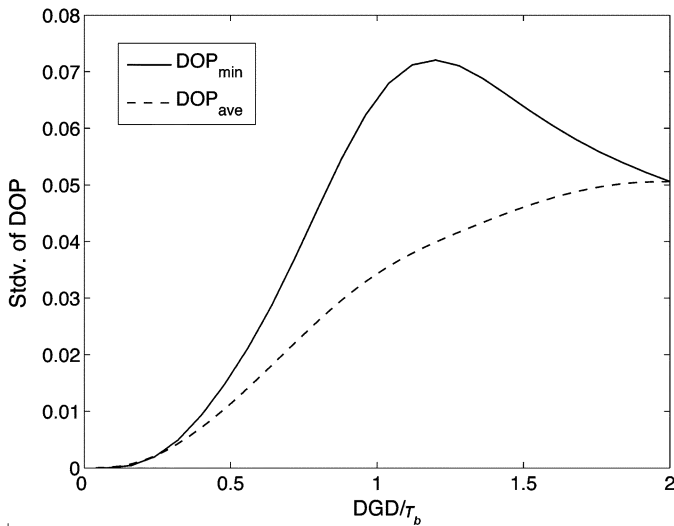


Fig. 7. Comparison of the standard deviation of the minimum and average DOPs versus DGD to the bit time in the presence of all-order PMD using NRZ input signal.

V. FIRST-ORDER FEEDFORWARD PMD COMPENSATION

A basic configuration for feedforward first-order PMD compensation [6] is shown in Fig. 8. The polarization state of an optical signal is scrambled before launching into a fiber and a compensator is adjusted according to the measured PMD parameters including PSPs and DGD at the output. Different methods were proposed to determine the PSPs of a fiber affected by PMD. In [8] and [15], PSPs' alignment using DOP-based control signals was investigated in a feedforward first-order PMD compensation system. In this paper, we only concentrate on the performance evaluation of DOP-based control signals in prediction of DGD and assume that the PSPs' alignment is ideally performed by the compensator. The compensator estimates DGD as a function of the feedforward control signal (DOP_{\min} or

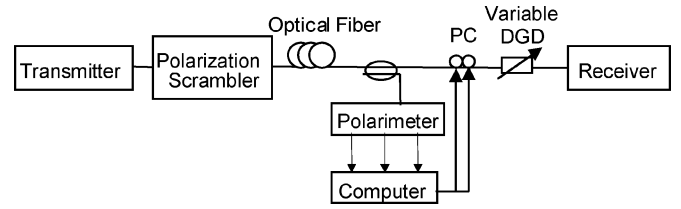


Fig. 8. Block diagram of a feedforward first-order PMD compensator.

DOP_{ave}) which is measured by polarimeter. This can be readily performed using the (DOP versus DGD) curves provided for the different data formats (i.e., RZ and NRZ) in Figs. 4 and 5. Note that polarization scrambling may lead to a timing jitter in the output signal. However, this effect can be significantly reduced by clock recovery techniques provided that the polarization scrambling frequency is sufficiently low [16]. Since PMD is a slowly varying phenomenon, the polarization scrambling frequency can be adjusted such that the clock recovery circuit eliminates the effects of timing jitter.

To have insight into the performance of the two DOP-based control signals in a first-order PMD compensator (Fig. 8), we calculate the outage probability of the system which quantifies the performance of the PMD compensator in case of severe pulse distortions. An outage happens whenever BER exceeds 10^{-12} . The BER is calculated using Gaussian statistics [17] and is optimized with respect to decision level and sampling time. To have fair comparison between different data formats (i.e., RZ and NRZ), we operate at 2-dB power margin above the receiver sensitivity at $\text{BER} = 10^{-12}$ for both data formats [1]. In this performance analysis, we take all orders of PMD into account using Orlandini's model described in Section IV. We launch PRBS-sequences (word length $2^5 - 1$) with Gaussian RZ pulses or super-Gaussian NRZ pulses into a PMD-induced fiber and detect the output sequences with an EDFA preamplified receiver. The EDFA noise figure and the optical filter bandwidth are assumed 3 dB and 1.4 nm, respectively. An electrical fifth-order Bessel filter with $0.5B$ bandwidth for RZ and $0.7B$ for NRZ signals is also used, where the bit rate B is 40 Gb/s. The input state of polarization is assumed constant during each data sequence as the data sequences length (~ 1 ns) is much shorter than the duration of a complete scrambling period over the Poincaré sphere. The scrambling period of typical polarization scramblers used for DGD monitoring is on the order of milliseconds [18]. However, several data sequences which are uniformly sampled during the scrambling period are considered for outage analysis. The DOP-based control signals can be readily calculated by measuring DOP using all of these data sequences at the receiver. Then the compensator is adjusted for the next scrambling period according to the measured DOP-based control signal and remains constant during the whole period. BER is then calculated for all the data sequences sampled during the scrambling period. Finally, all the BER values are taken into account to determine the outage probability

The calculation of outage probability is performed using a semianalytical method. A very large number of fiber realizations are required to produce the statistics of outage probability by this method. The fiber realizations are generated by varying the

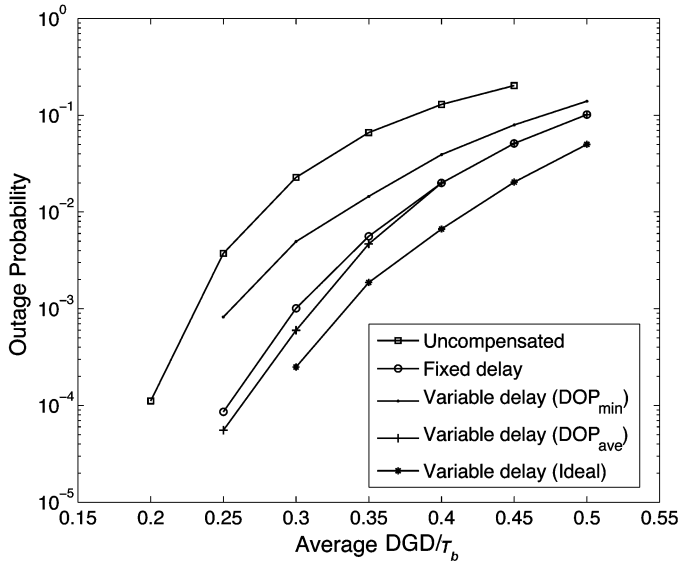


Fig. 9. Outage probability of the first-order DOP-based compensation systems for NRZ signals.

two parameters of Orlandini's model. Furthermore, the probability of occurrence of each fiber realization can be calculated using the joint probability density function of the two statistical parameters which is known by [13], [14]. Calculating BER for all fiber realizations with a certain average DGD and taking average over the BER outages with respect to the statistical parameters, yield the outage probability of the optical fiber link with the certain average DGD.

Figs. 9 and 10 show the outage probability of the two DOP-based compensation schemes (using DOP_{min} or DOP_{ave}) over the average DGD/T_b for NRZ and RZ data formats, respectively. As benchmarks, the outage probability of uncompensated system, a first-order compensation system with a fixed delay, and a first-order compensation system with a variable delay which is ideally adjusted to the exact instantaneous DGD are also included. In the fixed delay compensator, the delay is initially adjusted to the average DGD which can be computed before transmission by averaging over the measured DGD samples of the link.

For NRZ signals (Fig. 9), both DOP-based compensation schemes outperform the fixed delay compensation scheme which means that the control signals work properly. Although the performances of two DOP-based compensators are not close to the performance of ideal first-order PMD compensation, they are gradually converging to the ideal performance as average DGD decreases. It is also observed that using DOP_{ave} instead of DOP_{min} as the control signal improves gradually the performance of the system as the average DGD decreases which confirms the results of Section IV (Fig. 7). However, this improvement is not significant from the outage point of view, because the difference between the standard deviation of the two control signals is relatively small in the practical DGD range.

For RZ signals (Fig. 10), we observe that compensation using DOP_{ave} is still beneficial for low average DGDs as it outperforms the fixed delay compensation. However, the performance

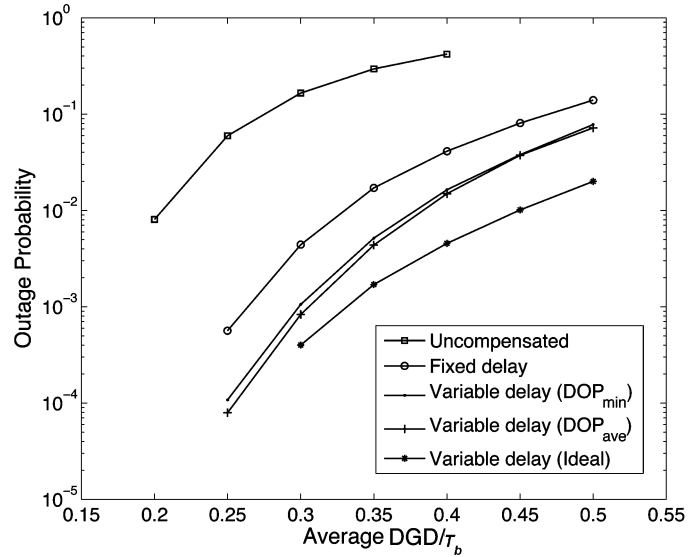


Fig. 10. Outage probability of the first-order DOP-based compensation systems for RZ signals.

of DOP_{min} as the control signal not only is worse than that of DOP_{ave} but even cannot provide the same performance as fixed delay PMD compensation. This observation can be explained by considering the high standard deviation of the DOP measurement samples for RZ pulses (Fig. 6) which causes a significant inaccuracy in predicting DGD. The ideal first-order PMD compensation again outperforms the other compensation techniques.

VI. CONCLUSION

The DOP of a scrambled signal propagating through an optical fiber affected by all-order PMD was derived. The average DOP was introduced as an alternative to minimum DOP which is the most common DOP-based control signal for DGD monitoring in PMD compensation systems. An analytical expression was determined for DOP_{ave} of a scrambled signal. The DOP-based DGD monitoring was evaluated in the presence of first- and all-order PMDs. The results show a higher order limit to DGD monitoring range in addition to the first-order limit which has been previously reported. Moreover, the comparison between the two control signals in terms of DGD monitoring range represented a new advantage of DOP_{ave} compared with DOP_{min} which is its wider DGD monitoring range. The performance of the two control signals were further evaluated by obtaining the outage probability of a first-order PMD compensator in a feedforward configuration. The results show that DOP_{ave} outperforms DOP_{min} for both RZ and NRZ signals.

APPENDIX

The analytical expressions of the output Stokes parameters, presented in [9], are obtained by comparing the definition of DOP in terms of Stokes parameters [see, for instance, (6)] with the expression obtained for DOP in [9]. However, there is an uncertainty in the sign of the Stokes parameters because in (6), DOP is defined in terms of the square of the Stokes parameters.

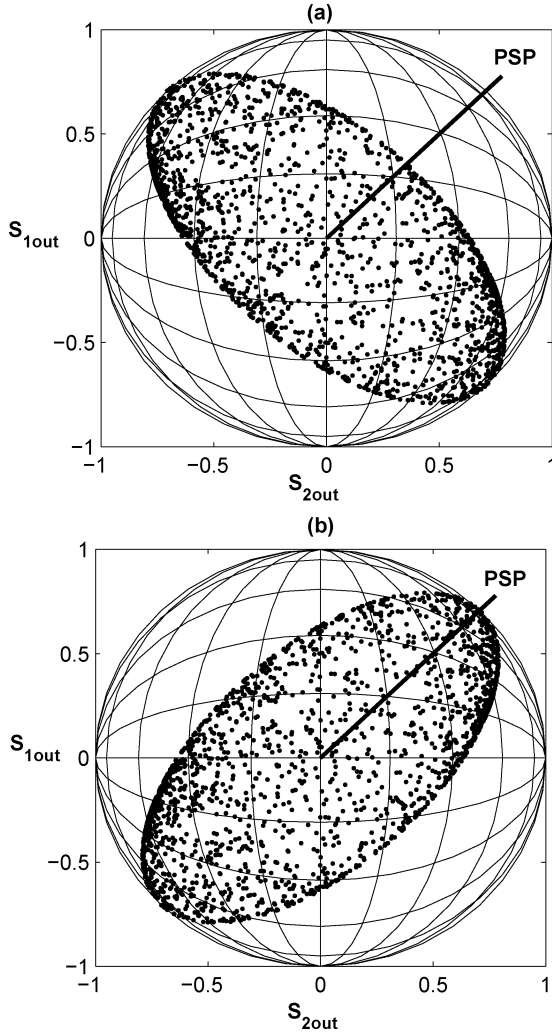


Fig. 11. The normalized output Stokes vectors for a scrambled signal obtained by (a) modified and (b) unmodified expressions of the Stokes parameters.

To investigate the correct sign of the Stokes parameters, we consider three fundamental input SOPs $[1 \ 0 \ 0]^T$, $[0 \ 1 \ 0]^T$, and $[0 \ 0 \ 1]^T$ in the Stokes space for a signal launched into a fiber. Taking into account only first-order PMD, we assume the fiber's fast PSP is aligned with the input SOP of the signal in each case. Hence the optical signal travels only along one polarization mode and the SOP of the signal remains unchanged at the output of the fiber. Therefore, the sign of each Stokes parameter can be verified by checking the output SOP for each case. The unitary matrix of the fiber $U(\omega)$ can be obtained as

$$U(\omega) = R^{-1}DR \quad (20)$$

where $D(\omega)$ is a diagonal matrix that takes into account the time delay between the two PSPs, described by

$$D(\omega) = \begin{bmatrix} e^{j\omega DGD/2} & 0 \\ 0 & e^{-j\omega DGD/2} \end{bmatrix} \quad (21)$$

and R the rotation matrix can be expressed as

$$R = \begin{bmatrix} \cos(\theta_r)e^{j\varphi_r} & -\sin(\theta_r) \\ \sin(\theta_r) & \cos(\theta_r)e^{-j\varphi_r} \end{bmatrix} \quad (22)$$

where the rotation angles θ_r and φ_r assumed to be zero for the first case to align the input SOP with the fast PSP. We also consider $\theta_r = \pi/4$ and $\varphi_r = 0$ for the second case and $\theta_r = \pi/4$ and $\varphi_r = \pi/2$ for the third case. The output Stokes vector of each case can be accordingly obtained using the unmodified and modified versions of (7)–(9) (i.e., before and after multiplying S_{2out} and S_{3out} by -1). The results show that the output SOP for the first case is the same as the input SOP. However, for the two other cases, the output Stokes vectors without modification are the opposites of the input Stokes vectors and it means that the signal is launched along the fast PSP but the output SOP is aligned with the slow PSP. Thus, S_{2out} and S_{3out} should be modified by reversing their sign.

Fig. 11(a) and (b) represent the normalized output Stokes vectors of a scrambled signal affected by first-order PMD before and after reversing the sign of S_{2out} and S_{3out} , respectively. The samples of the normalized output Stokes vector are obtained for 1000 independent input SOPs randomly generated over the Poincaré sphere. As it is observed in Fig. 11(b), the long axis of the DOP ellipsoid obtained by the modified expressions is aligned with the PSP of the fiber as reported in [4].

REFERENCES

- [1] H. Sunnerud, C. Xie, M. Karlsson, R. Samuelsson, and P. A. Andrekson, "A comparison between different PMD compensation techniques," *J. Lightw. Technol.*, vol. 20, pp. 368–378, Mar. 2002.
- [2] R. Noe, D. Sandel, M. Yoshida-Dierolf, S. Hinz, V. Mirvoda, A. Schopflin, C. Gungener, E. Gottwald, C. Scheerer, G. Fischer, T. Weyrauch, and W. Haase, "Polarization mode dispersion compensation at 10, 20, and 40 Gb/s with various optical equalizers," *J. Lightw. Technol.*, vol. 17, pp. 1602–1616, Sep. 1999.
- [3] H. Y. Pua, K. Peddanarappagari, B. Zhu, C. Allen, K. Demarest, and R. Hui, "An adaptive first-order polarization-mode dispersion compensation system aided by polarization scrambling: Theory and demonstration," *J. Lightw. Technol.*, vol. 18, pp. 832–841, Jun. 2000.
- [4] H. Rosenfeldt, C. Knothe, R. Ulrich, E. Brinkmeyer, U. Feiste, C. Schubert, J. Berger, R. Ludwig, H. G. Weber, and A. Ehrhardt, "Automatic PMD compensation at 40 Gbit/s and 80 Gbit/s using a 3-dimensional DOP evaluation for feedback," in *Proc. Conf. Opt. Fiber Commun.*, 2001, vol. 4, pp. PD27-1–PD27-3.
- [5] S. Kieckbusch, S. Ferber, H. Rosenfeldt, R. Ludwig, C. Boerner, A. Ehrhardt, E. Brinkmeyer, and H. G. Weber, "Automatic PMD compensator in a 160-Gb/s OTDM transmission over deployed fiber using RZ-DPSK modulation format," *J. Lightw. Technol.*, vol. 23, pp. 165–171, Jan. 2005.
- [6] P. C. Chou, J. M. Fini, and H. A. Haus, "Demonstration of a feed-forward PMD compensation technique," *IEEE Photon. Technol. Lett.*, vol. 14, pp. 161–163, Feb. 2002.
- [7] H. Rosenfeldt, R. Ulrich, E. Brinkmeyer, U. Feiste, C. Schubert, J. Berger, R. Ludwig, H. G. Weber, and A. Ehrhardt, "Feed-forward approach for automatic PMD compensation at 80 Gbit/s over 45 km installed single mode fiber," in *Proc. Europ. Conf. Opt. Commun.*, 2001, vol. 6, pp. 68–69.
- [8] P. C. Chou, J. M. Fini, and H. A. Haus, "Real-time principal state characterization for use in PMD compensators," *IEEE Photon. Technol. Lett.*, vol. 13, pp. 568–570, Jun. 2001.
- [9] S. M. Motaghian Nezam, J. E. McGeehan, and A. E. Willner, "Theoretical and experimental analysis of the dependence of a signal's degree of polarization on the optical data spectrum," *J. Lightwave Technol.*, vol. 22, pp. 763–772, Mar. 2004.
- [10] H. Miao and C. Yang, "Analysis of signal degree of polarization degradation induced by polarization-mode dispersion in optical fibers," *IEEE Photon. Technol. Lett.*, vol. 16, pp. 2475–2477, Nov. 2004.
- [11] S. Huard, *Polarization of Light*. New York: Wiley, 1997.
- [12] A. Orlandini and L. Vincetti, "A simple and useful model for Jones matrix to evaluate higher order polarization-mode dispersion effects," *IEEE Photon. Technol. Lett.*, vol. 13, pp. 1176–1178, Nov. 2001.
- [13] A. Orlandini and L. Vincetti, "Comparison of the Jones matrix analytical models applied to optical system affected by high-order PMD," *J. Lightwave Technol.*, vol. 21, pp. 1456–1464, Jun. 2003.

- [14] G. J. Foschini, L. E. Nelson, R. M. Jopson, and H. Kogelnik, "Statistics of second-order PMD depolarization," *J. Lightw. Technol.*, vol. 19, pp. 1882–1886, Dec. 2001.
- [15] M. Safari and A. A. Shishegar, "A simple and fast first-order PMD compensator using a polarizer," in *Proc. 5th Int. Conf. Opt. Commun. Netw./The 2nd Int. Symp. Adv. Trends in Fiber Optics and Appl. (ICOON/ATFO'06)*, China, Sep. 2006, pp. 282–285.
- [16] R. Salem, G. E. Tudury, T. U. Horton, G. M. Carter, and T. E. Murphy, "Polarization-insensitive optical clock recovery at 80 Gb/s using a silicon photodiode," *IEEE Photon. Technol. Lett.*, vol. 17, pp. 1968–1970, Sep. 2005.
- [17] G. P. Agrawal, *Fiber-Optic Communication Systems*. New York: Wiley, 1992.
- [18] A. E. Willner, S. M. R. M. Nezam, L.-S. Yan, Z. Pan, and M. C. Hauer, "Monitoring and control of polarization-related impairments in optical fiber systems," *J. Lightw. Technol.*, vol. 22, pp. 106–125, Jan. 2004.



Majid Safari (S'08) received the B.Sc. degree in electrical engineering from the University of Tehran, Tehran, Iran, in 2003 and the M.S. degree in electrical engineering from Sharif University of Technology, Tehran, in 2005.

He is currently pursuing the Ph.D. degree in electrical engineering at the University of Waterloo, Waterloo, Canada. His research interests include optical fiber communications and free-space optical communications.



Amir Ahmad Shishegar (S'98–M'03) received the B.Sc. degree (with honors), M.Sc., and Ph.D. degrees in electrical engineering from the University of Tehran, Tehran, Iran.

He was a visiting scholar with the University of Waterloo, Waterloo, Canada and Apollo Photonics Inc., Canada, during 1999 and 2000. He is currently an Assistant Professor with the Department of Electrical Engineering, Sharif University of Technology, Tehran. His research interests and activities include analytical and computational electromagnetics, electromagnetic wave propagation modeling, analysis and design of passive optical devices, and optical integrated circuits.